Preparation and Characterization of Dense Cellulose Film for Membrane Application

Muhammad Ichwan,[1] Tae-Won Son[2]

[1]*Department of Textile Engineering, Yeungnam University, Gyeongsan, Gyeongbuk 712-749, South Korea*
[2]*School of Textile, Yeungnam University, Gyeongsan, Gyeongbuk 712-749, South Korea*

Received 31 January 2011; accepted 14 June 2011
DOI 10.1002/app.35104
Published online 18 October 2011 in Wiley Online Library (wileyonlinelibrary.com).

ABSTRACT: Regenerated cellulose films were prepared with environmentally friendly process by utilized *N*-methylmorpholine-*N*-oxide (NMMO)-Cellulose system. To prepare a dense cellulose film for membrane application, some parameter process which influence porous forming such as cellulose DP, cellulose concentration, addition NMMO in coagulation bath, coagulation bath temperature, and drying condition were investigated. We resumed that the porosity and pore size of cellulose membrane decrease with lower cellulose DP, higher cellulose concentration, addition of NMMO in coagulation bath, applying room temperature in coagulation bath and drying, and applying vacuum on drying process resulted in membranes with porosity in range of 24–41% and pore size 13.4–20.2 nm. The main factor for controlling porosity and pore size of dense cellulose membrane was coagulation process condition especially addition of NMMO into coagulation bath. © 2011 Wiley Periodicals, Inc. J Appl Polym Sci 124: 1409–1418, 2012

Key words: cellulose; NMMO; membrane; dense; porosity

INTRODUCTION

In spite of the rapid development in synthetic polymer industries, cellulose and its derivatives are still holding an important position. As a kind of environmentally friendly and renewable resources that are available in abundant quantity, cellulose, a naturally occurring polysaccharide, has great potential to apply in some industrial sector. In the last three decades cellulose have been found to have extensive commercial applications in membrane separation processes include, microfiltration, ultrafiltration, nanofiltration, reverse osmosis, electrolysis, dialysis, electrodialysis, gas separation, vapor permeation, pervaporation, and membrane distillation.[1] The wide use of cellulose membrane recently is because of their relatively low cost, good compatibility with biological compounds, and their excellent hydrophilic properties.[2] Moreover utilizing cellulose as a raw material is a subtle way to save environment as well as to reduce consumption of the limited resource of our petroleum.[3]

The strong hydrogen bonds that occur between cellulose chains cause cellulose not to be dissolved in ordinary solvents. Thus, during the early development of cellulose membrane production, cellulose membrane is made by converting purified cellulose to a soluble derivative, such as xanthate (viscose process) or cuprammonium cellulose complex, and then precipitating from its coagulation and resulting membrane is given the name of Cellophane membrane or regenerated cuprammonium cellulose membrane.[4,5] However, as a result of the serious environmental problems inherent with the viscose process and low flux rate and rapid usage of cuproammonium cellulose membrane as well as cost problem induced by recovery of chemicals used, nowadays these two conventional methods development was greatly restricted.[6–8]

Therefore, the manufacturing methods that are environmentally safe and can be performed economically as well as high productivity have been pursued recently. Related to this, nowadays scientists are concern to a new solvent, *N*-methylmorpholine-*N*-oxide (NMMO), which can dissolve cellulose through a pure physical procedure.[9–12] NMMO has a strong electronegative oxygen atom that can break the hydrogen bonds between cellulose chains and form new hydrogen bonds with NMMO to produce viscous solution of cellulose.[12–14] The particular characteristic of the NMMO process is that it involves essentially physical phenomena, so that no chemical reaction takes place and no chemical by products are formed which must be disposed off as waste products or transformed back by chemical methods into the initial substances.[15,16]

The use of NMMO as the new organic solvent for cellulose opens up new perspectives for cellulose membrane development and its application in

Correspondence to: T.-W. Son (twson@yu.ac.kr).

TABLE I
Experimental Design Condition

Sample no.	Pulp DP	Pulp %	Coagulation bath	Drying
1	Mixed DP (50 : 50)	10%	20°C water	Vacuum 50°C
2	DP 850	10%	20°C water	Vacuum 50°C
3	DP 1200	10%	20°C water	Vacuum 50°C
4	DP 850	8%	20°C water	Vacuum 50°C
5	DP 850	11%	20°C water	Vacuum 50°C
6	DP 850	10%	20°C, 25 wt% NMMO	Vacuum 50°C
7	DP 850	10%	20°C, 50 wt % NMMO	Vacuum 50°C
8	DP 850	10%	40°C water	Vacuum 50°C
9	DP 850	10%	60°C water	Vacuum 50°C
10	DP 850	10%	20°C water	30°C
11	DP 850	10%	20°C water	50°C

separation processes. Practically, membrane separation processes differ based on separation mechanisms and size of the separated particles or also can be categorized based on their structure (morphology). Based on the membrane morphology, three such types of synthetic membranes are commonly used in separation industry such as dense membranes, porous membranes, and asymmetric membranes. Both dense and porous membranes have certain amount of pores. The formation of a pore can be induced by the dissolution of a "better" solvent into a "poorer" solvent in a polymer solution.[17] Other types of pore structure can be produced by stretching of crystalline structure polymers. The structure of porous membrane is related to the characteristics of the interacting polymer and solvent, components concentration, molecular weight, temperature, and storing time in solution. The thicker porous membranes provide support for the thin dense membrane layers forming the asymmetric membrane structures and such a kind of membrane with low porosity and pore size less than 50 nm is suitable for use in separation process of pressure flux.[17,18]

Related to this, Togawa and Kondo studied the change of morphological properties in drawing water-swollen cellulose films prepared from NMMO solution. Transparent films prepared by the slow coagulation showed good drawability, and their noncrystalline regions (more than 80%) as well as crystalline regions (less than 20%) were highly oriented by the drawing process.[19] Diamantoglou et al. prepared cellulosic dialysis membranes in the form of flat, tubular, or hollow fiber membranes by shaping a solution of cellulose in NMMO.[7,8] The purpose of the present work is to form cellulose membranes from NMMO solution which is suitable for pressure flux by studying the effects of cellulose membrane preparation parameters such as cellulose degree of polymerization, solution concentration, coagulation bath, and drying condition to the porosity properties and membrane performance.

EXPERIMENTAL

Materials

The cellulose used in this study was a softwood pulp with degree of polymerization of 850 and 1200 and α cellulose content more than 93%, supplied by Sappi. White crystal NMMO-monohydrate (with water content around 13.3%), which is in the form of fine powder was selected as solvent, *n*-Propylgallate (PG) supplied by Aldrich Chemical was used as antioxidant to avoid oxidation and degradation during the cellulose dissolving process.

Preparation of membranes

Two cellulose pulp samples with degree of polymerization (DP) 850 and 1200 are dried at 100°C in oven for 24 h before use. A certain amount of cellulose and NMMO monohydrate with the addition *n*-propylgallate (0.5 wt % from cellulose content) was placed in glass flask and gently stirred for 30 min to obtain homogeneous mixture. The dissolving of this mixture was carried out by heating at 110°C for 1 h under Nitrogen atmosphere. Cellulose NMMO solutions were cast into a membrane with a thickness of 30 μm on the glass plate then immersed into a coagulation bath for 24 h without any agitation. Coagulated membranes were washed with water of 30°C to remove the solvent completely. Finally, the samples were dried with different drying conditions. All the samples were prepared by above steps with some variation in condition process according to experimental design as summarized in Table I.

Apparatus and measurements

Water permeability

The membranes performances were characterized by dead-end filtration system. The pure water flux was measured under a pressure difference of 300 mmHg at ambient temperature by setting the membrane in apparatus as shown in Figure 1.The Flux rate, *FR*, is

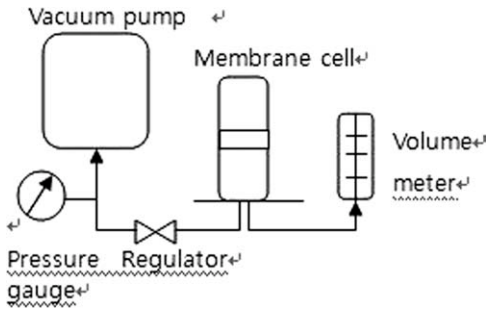

Figure 1 Water permeability analyzing apparatus.

calculated using eq. (1)[7,8] or as Permeation Flux, J as eq. (2)[3]:

$$\mathrm{FR} = \frac{V}{\mathbf{tSP}} \tag{1}$$

or

$$J = \frac{V}{tS} \tag{2}$$

in which V is the total volume of the water permeated during the experiment (mL); t is the operation time (h); and S is the membrane area (m^2), and P is test pressure (mmHg).

Membrane porosity

The porosity, P_r, of membranes was measured using an area of 16 cm^2 cut out squarely, by measuring the thickness, L (cm), and the dried weight (i.e., cellulose weight), W_d (g), using eq. (3):

$$Pr = 1 - \frac{W_d}{16L\rho} \tag{3}$$

where ρ is density of cellulose (1.561 g N cm^{-3} in this instance).

Membrane mean pore size

The mean pore radius, r_f (m), was evaluated by means of the water-flow-rate method by substituting the experimentally determined values of porosity, P_r as calculated by eq. (3) and permeation flux, J (m^3 m^{-2} s^{-1}) calculated by eq. (2), and thickness of dry membrane, L_d (m), into eq. (4), that was derived based on the straight through cylindrical pore model[20]:

$$rf. = \sqrt{\frac{8\eta_{H_2O} J L_d}{P_r \Delta P}} \tag{4}$$

in which η_{H2O} (N s m^{-2}) is the viscosity of water, and ΔP (N m^{-2}) is the load pressure. The thickness of each of the studied membranes was measured by using a micrometer graduated in 0.001-mm divisions.

Morphology properties

The cross-sectional morphology of membranes was examined with a scanning electron microscope. The samples were freeze-fractured in liquid nitrogen, followed by coating with gold in a sputtering device and observed by SEM instrument of *S*-4100.Hitachi, Japan at accelerating voltage 20 kV with 3000× magnification.

X-ray diffraction

X-ray diffraction was recorded at room temperature from 3° to 40° at a scanning speed of 2° min^{-1} with a Rigaku-D/Max-2200H diffractometer using Ni-filtered Cu Kα radiation of wavelength 0.1542 nm. The operating voltage and current were 40 kV and 30 mA, respectively. Crystalline of celluloses in samples were calculated from diffraction intensity data after treatment by using Peakfit software to determine the crystalline and amorphous area. The Peakfit use to deconvolute the diffraction profile which was fitted by Lorentzian function to find the peak intensity of 002 lattice and amorph phase. The crystallinity index was calculated by use equation proposed by Segal et al.[21]:

$$\mathbf{CrI} = \frac{I_{002} - I_{\mathbf{amorph}}}{I_{002}} \times 100\% \tag{5}$$

where CrI is crystallinity index, I_{002} is the maximum intensity of the (002) lattice diffraction and I_{amorph} is diffraction intensity at 18° 2θ. The average size of crystallite was calculated from the Scherrer equation with the method based on the width of the diffraction patterns obtained in the X-ray reflected crystalline region. In this study, the crystallite sizes were determined by using the diffraction pattern obtained from the 002 (*hkl*) lattice planes of cellulose film samples[22]:

$$\mathbf{D}_{(hkl)} = \frac{\mathbf{k}\lambda}{\mathbf{B}_{(hkl)}\cos\theta} \tag{6}$$

where (*hkl*) is the lattice plane, $D_{(hkl)}$ is the size of crystallite, k is the Scherrer constant (0.84), λ is the X-ray wavelength (0.154 nm), $B_{(hkl)}$ is the FWHM (full width half maximum) of the measured *hkl* reflection and θ is the corresponding Bragg angle (reflection angle).

Thermal properties/DSC

To learn the thermal properties of membrane, about 2.0 mg of the samples were weighted and sealed in aluminum pans. The thermal properties were

TABLE II
Water Permeability and Porosity Properties of Cellulose Film

Exp. code	Sample no.	Exp. condition	FR = flux rate (mL) h m^{-2} mmHg	Porosity (%)	2 r_f = pore size (nm)
A	1	mix DP	47.67 ± 6.27	40.6 ± 3.4	16.07 ± 1.24
	2	DP 850	40.63 ± 5.33	36.8 ± 3.2	14.23 ± 1.70
	3	DP1200	45.90 ± 6.16	41.4 ± 3.9	15.62 ± 1.82
B	4	8%	51.23 ± 6.15	38.2 ± 3.5	19.15 ± 2.25
	2	10%	40.63 ± 5.33	36.8 ± 3.2	14.23 ± 1.70
	5	11%	36.53 ± 4.81	31.3 ± 3.6	13.38 ± 1.67
C	2	water	40.63 ± 5.33	36.8 ± 3.2	14.23 ± 1.70
	6	nmmo 25%	31.90 ± 4.15	27.2 ± 2.6	14.39 ± 2.12
	7	nmmo 50%	28.17 ± 3.43	24.1 ± 2.5	14.33 ± 1.95
D	2	bath 20°C	40.63 ± 5.33	36.8 ± 3.2	14.23 ± 1.70
	8	bath 40°C	37.10 ± 4.39	23.6 ± 3.3	18.03 ± 1.75
	9	bath 60°C	38.33 ± 4.43	26.3 ± 3.5	20.20 ± 2.32
E	10	Dry 30°C	36.03 ± 5.17	25.6 ± 2.6	16.73 ± 1.02
	11	Dry 50°C	37.13 ± 5.21	27.7 ± 3.2	18.21 ± 1.34
	2	Vacuum dry 30°C	40.63 ± 5.33	36.8 ± 3.2	14.23 ± 1.70

obtained from 0 to 400°C at the heating rate of 10°C min^{-1} in a differential scanning calorimeter (TA Instrument 2010 DuPont, U.S.A).

Mechanical properties

The mechanical property of membrane was examined by Tenacity. The 10 cm × 1 cm samples were prepared in standard condition (20°C ± 1°C, 65% ± 2% humidity) for 24 h and ready to measure by Instron 3345 with test parameter of 25 kgf load cell and 20 cm min^{-1} tensile speed. Each sample was measured and average value was calculated.

Hydrophilic property

The hydrophilic property of membrane was studied based on the contact angle analysis measure by goniometer. Contact angle analysis measures the surface tension of water droplet at its interface with a homogenous surface by utilized static drop technique. The contact angle data was collected from average value of five measurements.

RESULTS AND DISCUSSION

The data given in Table II report the water permeability/flux (mL h^{-1} m^{-2} $mmHg^{-1}$), porosity (%) and the overall mean pore size (nm) of the cellulose membranes fabricated from casting solutions under different conditions, such as the degree of polymerization (DP) of cellulose pulp (Exp. code A), the cellulose concentration of casting solution (Exp. Code B), NMMO concentration in coagulation bath (Exp. code C), coagulation bath temperature (Exp. Code D), and drying condition (Exp. Code E).These data are an average value of repeat measurement obtained from different batch of membrane preparation.

Membrane porosity properties

The effect of pulp DP

Table II shows the pulp with higher DP (Exp. Code A) result in membrane which has higher porosity and water permeability properties. We have measured the viscosity of cellulose dope at 110°C using Brookfield viscometer for Samples 1, 2, and 3. Based on result shown in Table III, the higher DP (Samples 1 and 3) shows higher viscosity. Polymer with high degree of polymerization has longer chain and larger molecule compared to a polymer with low degree of polymerization. Therefore the high DP gives rise to entanglement among polymer chains, and then restricts molecule chain mobility to cause NMMO difficult to break hydrogen bond of cellulose during dissolution process result in less homogenous casting solution. Moreover the entangled polymer possibly avoids polymer chain to arrange closer to each other during coagulation process that induce more porous part on membrane. However when membrane is composed of mixed DP the porosity is slightly decreased as the low DP can reduce this effect which tends to give a slightly bigger pore size.

The effect of cellulose concentration in casting solution

The polymer concentration of the casting solution is the key factor affecting membrane performance such

TABLE III
Viscosity of Cellulose Dope Solution

Samples	Viscosity (cPs)	SD
1	782	66
2	514	6
3	981	22

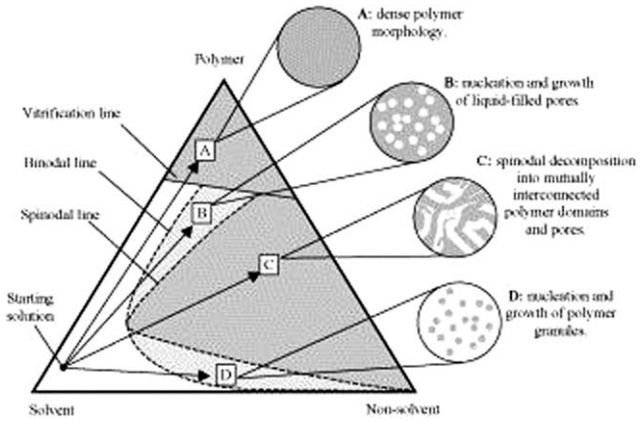

Figure 2 Ternary phase diagram in coagulation process of membrane.

as the permeation rate, rejection, and mechanical properties of membranes.[23] However this is restricted by process ability as well as production cost when higher concentration is applied. In this work we use 11 wt % of casting solution as maximum because at higher concentration the casting solution is too viscous to obtain an even membrane by film casting method. Data in Table II (Exp. B) shows that with increasing cellulose concentration from 8 to 11%, the porosity, pore size, and water permeated (flux) tend to decrease. This can be explained by increasing polymer concentration, which is related to increase in polymer chain amount per unit area, hence there is decrease in the free space (pore) in membrane and give smaller mean pore size.

The effect of NMMO in coagulation bath

Based on the data presented in Table II (Exp. Code C), it was found that the porosity is decrease from 36.8 to 24.1% while mean pore size is slightly decrease when the NMMO wt % content in coagulation bath temperature increases from 0 (water only) to 50 wt % NMMO. The formation of a pore can be induced by the dissolution of a "better" solvent into a "poorer" solvent in a polymer solution and can be divided by two different mechanisms, that is nucleation growth mechanism (NG) and spinodal mixing (SD) as demonstrated by Routes B and C of Figure 2, respectively.[24] This membrane is considered as result of the NG mechanism for the slow solidification process and the uniform dense structure as shown in Figure 3(f). When the cellulose/NMMO solution is immersed into NMMO/water, liquid–liquid phase separation occurs between NMMO as better solvent and water as poor solvent. The exchange rate of solvent and poor-solvent is slowed by NMMO in coagulation bath so as when entering the metastable region between binodal and spinodal line, nuclei are formed in the polymer solution. These nuclei grow into droplets until they touch each other and coalesce or until their growth is stopped by the solidification of the surrounding polymer solutions. Thus the polymer-poor phase grows into pores and the polymer-rich phase develops into a matrix.[25] In this case, the nucleation and growth mechanism can progress for some time before the solidification of the polymer-rich phase because the solidification rate is slow due to the low exchange rate of NMMO and water. Therefore addition of NMMO to coagulation bath will slower the diffusion rate and allow nuclei to grow homogenously to yield denser and smaller pore size of membrane structure.

The effect of coagulation bath temperature

Different coagulation bath temperatures affect the porosity and pore size of cellulose membranes. Increasing of coagulation bath temperature from 20 to 60°C resulted in lower porosity but bigger pore size. This can be explained by mechanism of the membrane formation suggested by Smolders and coworkers[26]: the top skin layer, where most likely gelation takes place, is caused by direct desolvation and the liquid–liquid phase separation is responsible for substructure morphology. The formation of pores in asymmetric membranes is controlled by the exchange of solvent in the polymer solution and nonsolvent in coagulation bath which is categorized as the nucleation and growth mechanism (NG) or to spinodal demixing (SD).[24,27–30] This membrane is believed to be the result of SD mechanism as described by Route C of Figure 2, because the coagulant is pure water so the exchange rate between NMMO and water is very rapid, moreover, accelerated by high temperature of coagulation bath. The nonsolvent diffuses quickly and passes the spinodal line before nucleation takes place. Thus, the spinodal decomposition may be stopped instantly to cause polymer-poor phase merge and formed macro voids at the direction of the thickness result in bigger pore size.[31] However, in the case of a lower temperature, the solvent-coagulant exchange rate is slower at the beginning of the precipitation and due to the large differential concentration between the solvent and the nonsolvent, the water diffuses quickly at the upper side of the solution resulting in the solidification of the dense skin layer, whereas the solvent has not enough driving force to diffuse through the dense skin as a result of the lower temperature. Thus the polymer-rich phase under the skin layer has enough time to merge resulting in smaller pore size of membrane structure.

The effect of drying condition

Data in Table II show that cellulose membrane process by drying at 30°C results in lower porosity

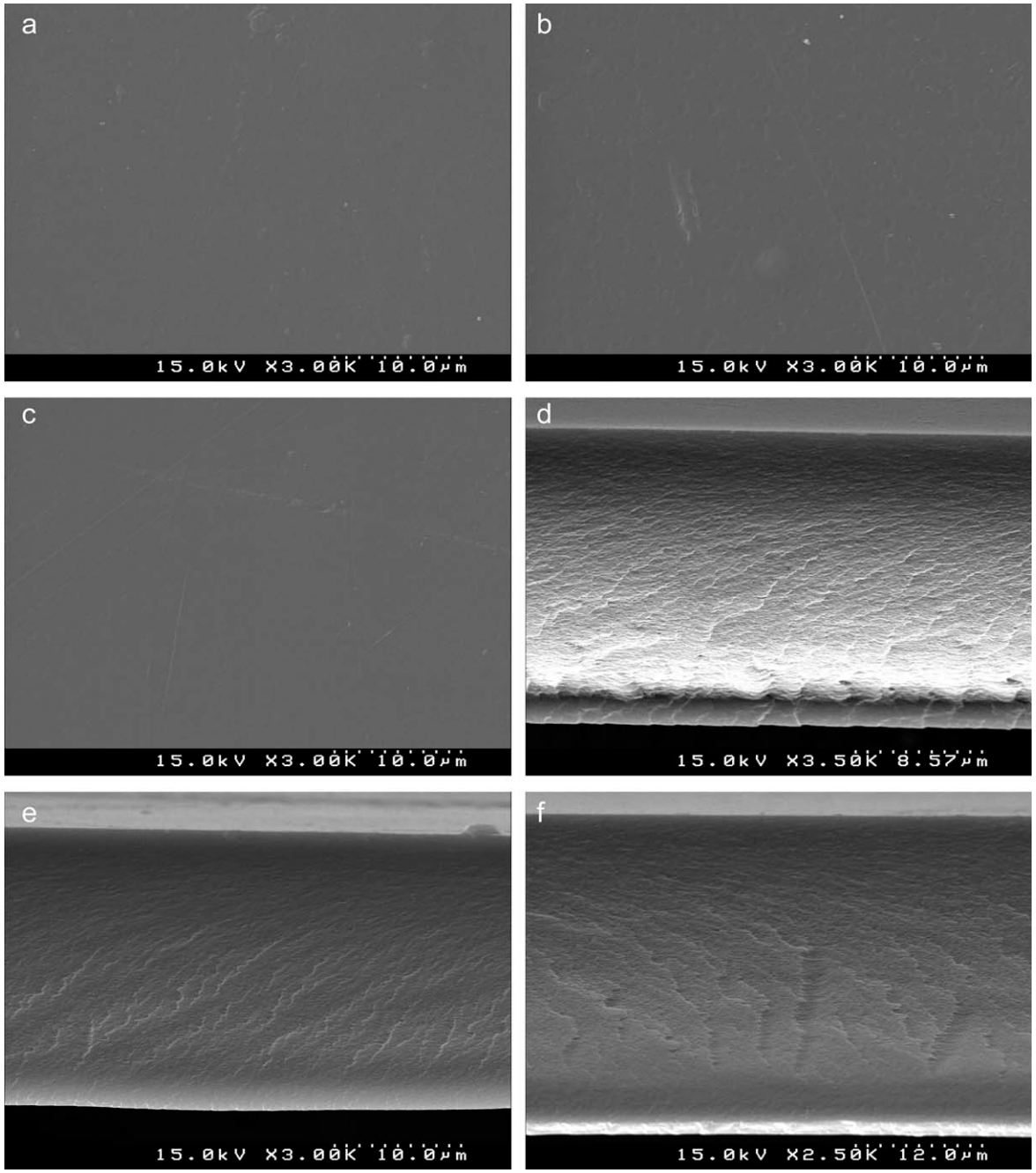

Figure 3 SEM photographs showing morphology of cellulose film prepared by different conditions. (a), (d) correspond to surface and cross section of Sample 2; (b), (e) correspond to surface and cross section of Sample 5, and (c), (f) correspond to surface and cross section of Sample 7.

(more dense) and smaller mean pore size than drying at 50°C. Vacuum condition applied during drying process result in smaller mean pore size of cellulose membrane. To explain the morphology changes during drying with different methods observed above, assumptions involved in the drying processes of cellulose membrane in this study were given as follows: during coagulation process, the solvent (NMMO) is diffused out and replaced by nonsolvent (water), and later this water could exist in two states: bonded water and free water.[12] The bonded water formed strong hydrogen bonds with cellulose molecules and the free water being surrounded by the bonded water had no contact with cellulose molecules. In the naturally drying process, the free water evaporated while the bonded water remained; the hydrogen bonds of water–water and water–cellulose were strong enough to pull cellulose in the region of macrovoids approaching closer and closer until new hydrogen bonds between cellulose chains were formed as the free water evaporated gradually. As a consequence, the macrovoids is reduced which

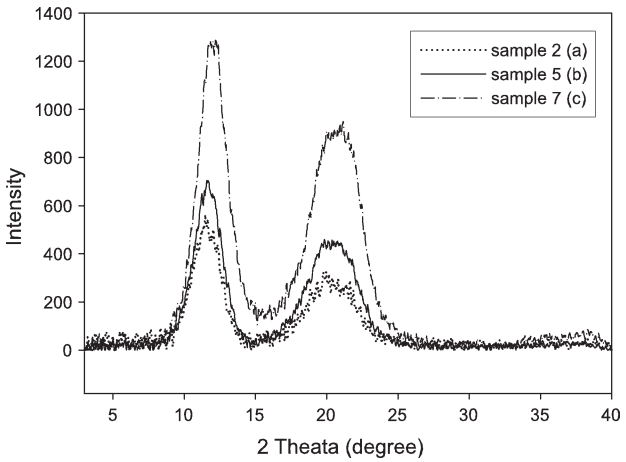

Figure 4 X-ray diffractogram of (a) Sample 2, (b) Sample 5, and (c) Sample 7.

result in smaller pore size and denser structure. On the other hand, higher drying temperature cause the free water inside the membrane to evaporate quickly, thus reduce the ability of macrovoids to approach closer to each other resulting in larger pore size. In addition, the vacuum pressure applied in drying possibly has forced the pore to shrink and result in smaller pore size.

Morphology properties

Figure 3 shows scanning electron micrographs of surface and cross section of the cellulose membrane prepared by this work from some different process conditions. By applying 3.00 K of magnification it revealed that the cellulose films generally present smooth surfaces with transparent appearance, however for higher concentration of cellulose concentration the smoothness is slightly decreased [Fig. 3(b)] and no significant difference can be seen for surface of cellulose membrane coagulation with water only [Fig. 3(a)] and 50 wt % NMMO as coagulation bath. The cross section of cellulose membrane confirms that these membranes are homogeneous which gradually decrease the dense structure from upper skin layer to support and bottom layer [Fig. 3(d–f)]. It can be seen that for higher cellulose concentration [Fig. 3(e)] and cellulose membrane coagulate with NMMO [Fig. 3(f)] that have more dense structure compared to lower cellulose concentration [Fig. 3(d)]. It is difficult to observe pore of cellulose membrane from the cross section of scanning micrograph magnification as the pore size range between 13 and 20 nm.

X-ray diffraction analysis

Figure 4 shows the X-ray diffractograms of cellulose membrane samples from different process conditions. The data is analyzed by using Peakfit software to determine the peak and intensity of crystalline and amorphous. The X-ray diffraction of (a) Sample 2, (b) Sample 5, and (c) Sample 7 showed peaks at 2θ around 12° for (101) and 19.5°–21° for (101) and (002), respectively, which are characteristic patterns for crystal cellulose II.

Table IV shows the crystallinity of membranes calculated from the X-ray diffractograms data by eq. (5) which revealed that CrI is in the range of 44–61%. The higher cellulose casting solution [Fig. 3(b)] and addition of NMMO into coagulation bath [Fig. 3(c)] significantly increased the crystallinity of cellulose membranes. The degree of crystallinity was increased with the concentration of cellulose. The increase of cellulose concentration affected the chain entanglement and polymer chain amount per unit area, thus increasing the ordered part in cellulose membranes. The degree of crystallinity was also increased with NMMO concentration, because the slower diffusion of NMMO is from inside the film to the coagulation bath and as consequent slower coagulation occurred with concentration of NMMO in the coagulation bath. The crystal size of Sample 2 is higher than Samples 5 and 7, while its crystallinity is lower than another two samples, this is possibly due to the 10% of cellulose contained in casting solution are distributed to smaller matrix film area (Sample 2 has more porosity) so as the amount of molecule per unit matrix area is higher which results in bigger crystal size.

Thermal properties

Figure 5 shows the DSC thermograms of the cellulose membrane with different cellulose DP. In the calorimetric study by DSC (in which samples were heated to temperatures reaching 400°C), several processes associated with water desorption and polymer decomposition were observed. At low temperatures, an endothermic process was detected, with a maximum occurring at ~ 86°C. This process is associated with water desorption and is caused by the hydrophilic behavior of cellulosic polymers. Moreover, a broad exothermic peak appears between 290 and 345°C. The onset temperature of the decomposition (T_d) and the maximum heat flow/mass (Q_{dmax}) with the associated temperature (T_{dmax}) of the different cellulose samples are compared in Table V. In this process, higher onset and maximum

TABLE IV
Crystallinity and Crystallite Size of Cellulose Film

Samples	Crystallinity (%) (CrI)	$D_{(002)}$ (nm)
2	44.58	0.74
5	56.54	0.23
7	61.98	0.32

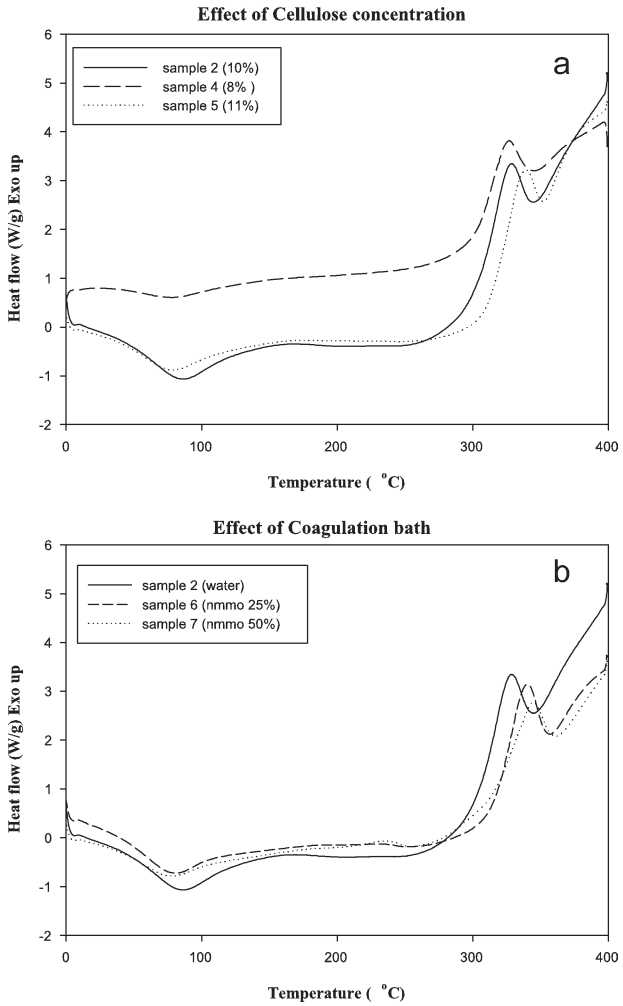

Figure 5 DSC curve of cellulose membranes (a) effect of cellulose concentration in casting solution; (b) effect of NMMO in coagulation bath.

decomposition temperatures are associated with higher thermal stability.[32] On the basis of DSC scans resumed in Table IV, we can see that T_d onset of cellulose with DP 1200 and DP 850 is the same whereas higher for mixed DP of cellulose membrane. Also, increasing in cellulose concentration, % NMMO in coagulation bath, coagulation bath temperature, and slow drying process results in higher T_d onset. The T_d onset and T_d max of thermal decomposition could be related to the crystallinity degree as well as the ordered structure, that yield in more compact and dense structure as increase in either property are associated with increases in their thermal resistance. The higher molecular orientation degree results in an improvement in the thermal behavior of membrane. In addition, the values for the maximum heat flow ($Q_{d\max}$) indicate that the membrane structure has less crystalline and less ordered structure, which favors the thermal decomposition process. The Samples 8 and 11 have low $Q_{d\max}$ value, presumably because the film has relative dense structure as

TABLE V
Characteristic Parameter of Thermal Decomposition of Cellulose Membrane Obtained from DSC Scans

Note	Sample no.	T_d max (°C)	$Q_{d\max}$ (W g^{-1})	T_d onset (°C)
dp mix	1	331	3.94	295
dp 850	2	328	3.36	289
dp 1200	3	325	3.46	289
8%	4	327	3.82	295
11%	5	340	3.22	295
25% nmmo	6	340	3.15	300
50% nmmo	7	345	2.77	300
bath 40°C	8	337	2.11	291
bath 60°C	9	334	2.86	291
dry 30°C	10	336	2.86	306
dry 50°C	11	338	2.10	310

describe by their porosity, pore size, and flux rate data. The higher $Q_{d\max}$ of mix DP is likely caused by inhomogen of film structure formed by mix of low and high molecular weight of cellulose. We assume that the shorter molecule form the ordered structure of film while the longer molecule formed the less order one. It needs higher temperature to completely decompose the less order structure of longer molecule compared to less order structure of short molecule as in Sample 2, moreover it releases more heat (higher $Q_{d\max}$) due to decomposition of higher molecule weight.

Mechanical properties

The tensile properties of the cellulose membrane were measured using a mechanical test instrument. Table VI shows the tenacity and tensile strain of 10 wt % (Sample 2) and 11 wt % (Sample 5) of cellulose concentration in casting solution and NMMO 50 wt % in coagulation bath (Sample 7).The measurements were conducted in 10 samples of each cellulose membranes. Table V summarizes the mechanical properties obtained including the tensile modulus (E) and the tenacity and strain (ε_f) at failure. The cellulose membrane of high cellulose concentration evidenced higher tenacity than those of lower cellulose concentrations and so does for cellulose membrane coagulate in bath of NMMO 50 wt %. We believe that the higher tenacity of these cellulose membranes are caused by higher degree of crystallinity of membrane as confirmed by data of crystallinity

TABLE VI
Mechanical Properties of Cellulose Membranes

Sample no.	Tensile strength (Mpa)	Strain at break (ε_f) (%)	Tensile modulus (E) (GPa)
2	47.80 ± 9.13	7.97 ± 3.19	0.64 ± 0.15
5	67.14 ± 11.23	7.37 ± 2.29	0.96 ± 0.22
7	50.46 ± 9.96	6.76 ± 2.22	0.75 ± 0.17

TABLE VII
Contact Angle of Cellulose Membranes

Sample no.	Contact angle (°)
2	40 ± 1.6
5	24 ± 2.1
7	28 ± 2.2

(Table IV) and DSC data (Table V). These data also show that both samples were stiffer with lower strain at failure as consequence of its higher ordered and denser structure of cellulose membranes.

Hydrophilic properties

Cellulose membrane possesses a strong hydrophilic property and thus has lower contact angle. Accordingly, Table VII and Figure 6 displays that the contact angle of cellulose membrane decreases as cellulose concentration in casting solution (Sample 5) and NMMO in coagulation bath (Sample 7) increases. Its strong hydrophilic property is generated by hydroxyl groups in cellulose molecule that can attract water molecule and cause contact angle of surface observed at below 90°. Moreover, Wenzel postulated that when the hydrophilic material has

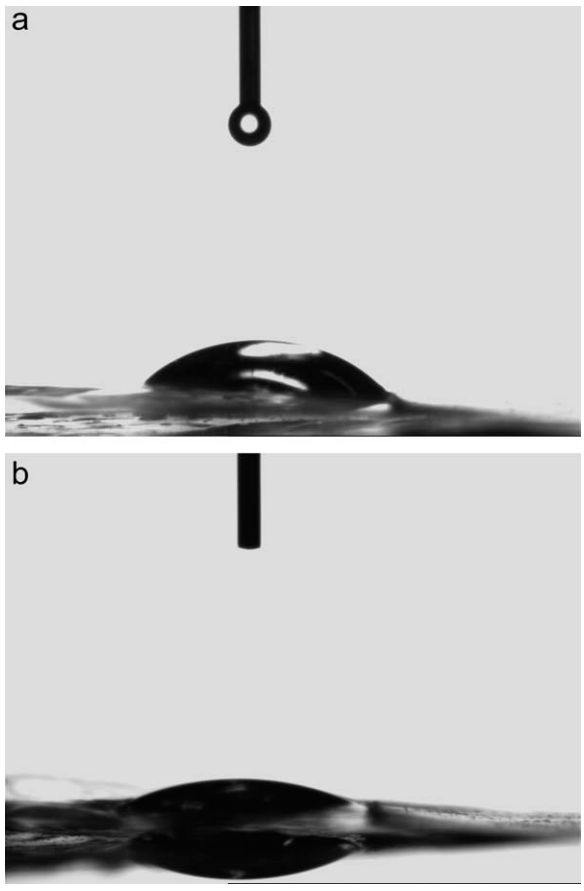

Figure 6 Contact angle of cellulose membrane (a) Sample 2 and (b) Sample 7.

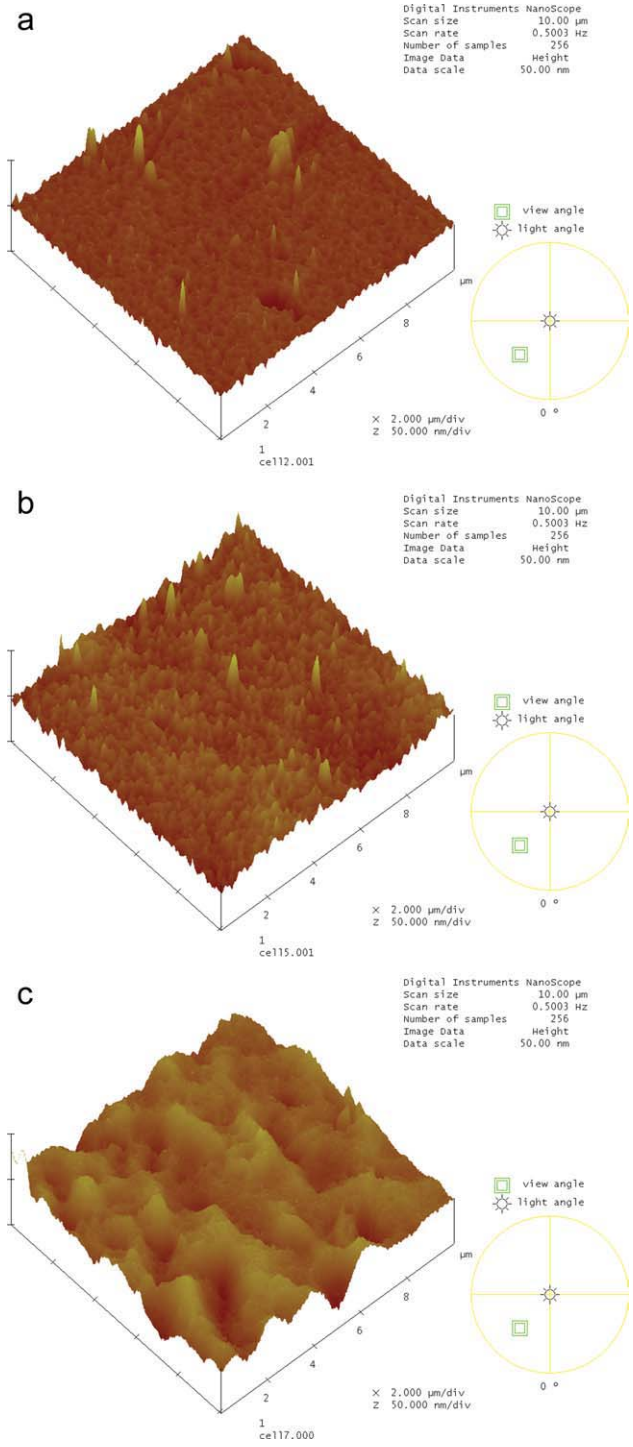

Figure 7 AFM surface profile of membrane (a) Sample 2, (b) Sample 5, (c) Sample 7. [Color figure can be viewed in the online issue, which is available at wileyonlinelibrary.com.]

rough surface, this kind of surface will decrease the contact angle. Related to this the increase of cellulose concentration in casting solution and addition of NMMO in coagulation bath results in rougher surface as confirmed by Figure 7(b–c) and data in Table VIII. These can be explained at higher concentration and by addition of NMMO.

TABLE VIII
Roughness Analysis of Cellulose Membranes

Sample no.	Roughness (nm)
2	2.17 ± 0.15
5	3.48 ± 0.25
7	6.31 ± 0.47

CONCLUSIONS

Dense cellulose films for membrane application were successfully prepared through simple and environmentally friendly process from *N*-methylmorpholine *N*-oxide solution of cellulose with various conditions that resulted in dense asymmetric membrane structure composed of a skin and porous support layer.

For a given condition the porosity and pore size decrease with lower cellulose DP, higher cellulose concentration, additional NMMO in coagulation bath, room temperature of coagulation bath, drying at room temperature, and applying vacuum on drying process, which have membrane porosity still in range of 24–41% and pore size from 13.4 to 20.2 nm.

We resumed that the main factor for controlling porosity and pore size of dense cellulose membrane was coagulation process condition especially addition of NMMO into coagulation bath.

References

1. Pinnau, I.; Freeman, B. D. Membrane Formation and Modification; Am Chem Soc: Washington, 1999.
2. Yang, G.; Zhang, L. N. J Membr Sci 1996, 114, 149.
3. Zhang, Y.; Shao, H.; Wu, C.; Hu, X. Macromol Biosci 2001, 1, 141.
4. Kamide, K.; Iijima, H. Recent Advances in Cellulosic Membranes; Hanser: Munich, 1994; Chapter 10, p 189.
5. Wu, J.; Yuan, Q. J Membr Sci 2002, 204, 185.
6. Simon, J.; Muller, H. P.; Koch, R.; Muller, V. Polym Degrad Stab 1998, 59, 107.
7. Diamantoglou, M.; Nywlt, M.; Holz, W. US Patent 6,019,925, 2000.
8. Akzo Nobel NV, invs. Chem Abstr 1998, 128, 66541v.
9. Bang, Y. H.; Lee, S.; Park, J. B.; Cho, H. H. J Appl Polym Sci 1999, 73, 268.
10. Abe, Y.; Mochizuki, A. J Appl Polym Sci 2002, 84, 2302.
11. Lewandowski, Z. J Appl Polym Sci 2002, 83, 2762.
12. Jiea, X.; Caoa, Y.; Qinb, J. J.; Liua, J.; Yuan, Q. J Membr Sci 2005, 246, 157.
13. Maia, E.; Peguy, A.; Perez, S. Acta Cryst 1981, B37, 1858.
14. Berger, W.; Keck, M.; Philipp, B. Cell Chem Technol 1988, 22, 387.
15. Andresen, E. M.; Mitchell, G. R. Polymer 1998, 39, 7127.
16. Chanzy, H.; Dube, M.; Marchessault, R. H. J Polym Sci Polym Lett 1979, 17, 219.
17. Osada, Y.; Nakagawa, T. Membrane Science and Technology; Marcel Dekker: New York, 1992.
18. Vieth, W. R. Diffusion in and through Polymers; Hanser Verlag: Munich, 1991.
19. Togawa, E. J.; Kondo, T. J Polym Sci Polym Phys Ed 1999, 37, 451.
20. Iijima, H.; Iwata, M.; Inamoto, M.; Kamide, K. Polym J 1997, 29, 150.
21. Segal, L.; Creely, L.; Martin, A. E.; Conrad, C. M. Textile Res J 1959, 29, 786.
22. Ahtee, M.; Hattula, T.; Mangs, J.; Paakkari, T. Paperi Ja Puu 1983, 8, 475.
23. Jian, X. G.; Dai, Y.; He, G. H.; Chen, G. H. J Membr Sci 1999, 162, 187.
24. Laity, P. R.; Glover, P. M.; Hay, J. N. Polymer 2002, 43, 5827.
25. Kim, J. Y.; Lee, H. K.; Kim, S. C. J Membr Sci 1999, 163, 164.
26. Koenhen, D. M.; Mulder, M. H. V.; Smolders, C. A. J Appl Polym Sci 1997, 21, 199.
27. Machado, P. S. T.; Habert, A. C.; Borges, C. P. J Membr Sci 1999, 155, 171.
28. Reuvers, F. W.; Altena, C. A.; Smolders, C. A. J Polym Sci Polym Phys Ed 1986, 24, 793.
29. Reuvers, A. J.; Van den Berg, J. W. A.; Smolders, C. A. J Membr Sci 1987, 34, 45.
30. Cheng, L. P.; Soh, Y. S.; Dwan, A.; Gryte, C. C. J Polym Sci Polym Phys Ed 1994, 32, 1413.
31. Smolders, C. A.; Reuvers, A. J.; Boom, R. M.; Wienk, L. M. J Membr Sci 1992, 73, 259.
32. Carrillo, F.; Colom, X.; Sunol, J. J.; Saurina, J. Eur Polym J 2004, 40, 2229.